

Supporting Information

© Wiley-VCH 2014

69451 Weinheim, Germany

**A De Novo Designed Metalloenzyme for the Hydration of CO<sub>2</sub>\*\***

*Virginia M. Cangelosi, Aniruddha Deb, James E. Penner-Hahn, and Vincent L. Pecoraro\**

ange\_201404925\_sm\_miscellaneous\_information.pdf

## Supporting Information

### Table of Contents

|                            |         |
|----------------------------|---------|
| Figure S1.....             | Page S2 |
| Figure S2.....             | Page S2 |
| Figure S3.....             | Page S3 |
| Figure S4.....             | Page S3 |
| Figure S5.....             | Page S4 |
| Figure S6.....             | Page S4 |
| Table S1.....              | Page S4 |
| Experimental Section ..... | Page S5 |

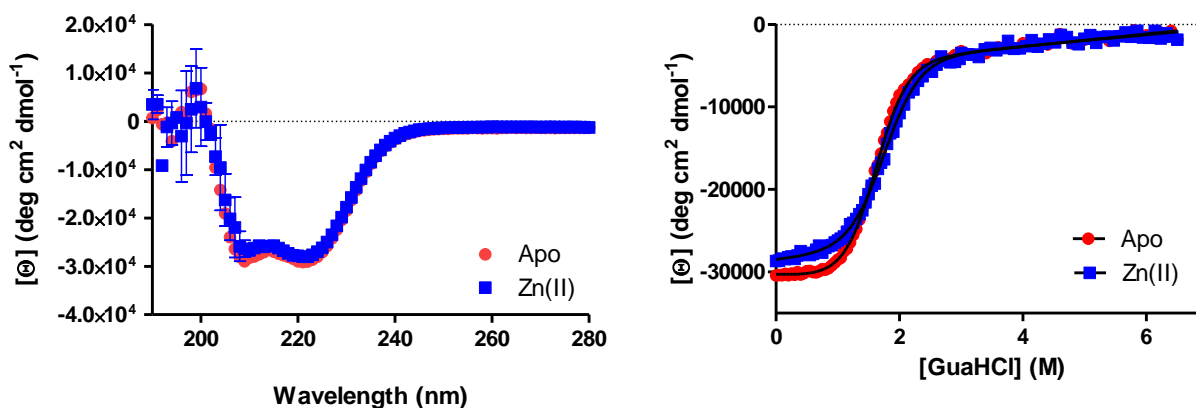


**Figure S1.** Circular dichroism spectroscopy for 5  $\mu\text{M}$   $\alpha_3\text{DH}_3$  (red) and 5  $\mu\text{M}$   $\text{Zn(II)}\alpha_3\text{DH}_3$  (blue) at pH 9.0. Left: Spectra showing  $\alpha$ -helical nature of fully-folded peptides. Apo- $\alpha_3\text{DH}_3$  and  $\text{Zn(II)}\alpha_3\text{DH}_3$  are initially 82% and 83% folded, respectively. Right: Guanidine hydrochloride denaturations. Fittings reveal  $\Delta G_u = 3.4$  kcal/mol for apo-  $\alpha_3\text{DH}_3$  and 3.5 kcal/mol for  $\text{Zn(II)}\text{-}\alpha_3\text{DH}_3$ .

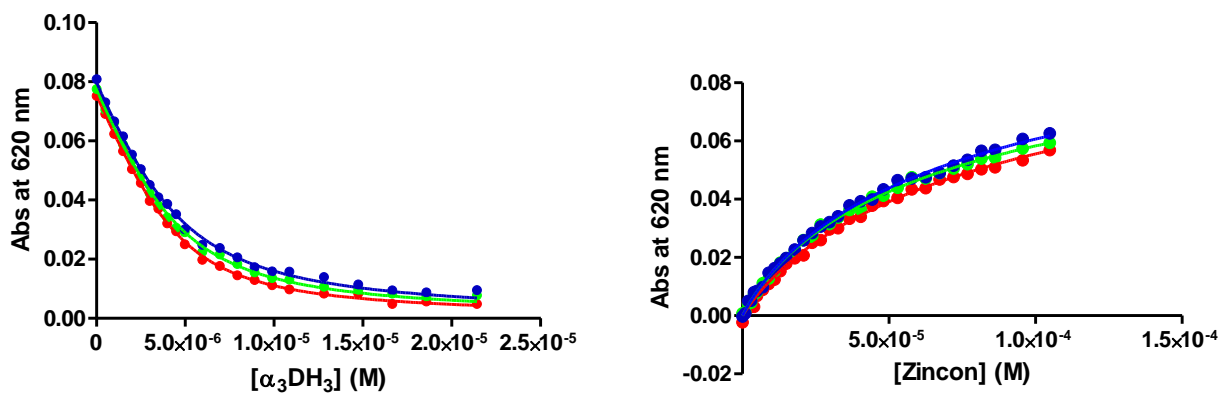


**Figure S2.** Competitive Zincon binding titrations at pH 7.5 with  $\alpha_3\text{DH}_3$ . In triplicate, plots show the absorbance of  $\text{Zn(II)}\text{-Zincon}$  at 620 nm plotted against the titrant concentration. Left: Titration of  $\alpha_3\text{DH}_3$  into  $\text{Zn(II)}\text{-Zincon}$  (10  $\mu\text{M}$  Zincon, 5  $\mu\text{M}$   $\text{ZnSO}_4$ , 50 mM HEPES). Right: Titration of Zincon into  $\text{Zn(II)}\alpha_3\text{DH}_3$  (10  $\mu\text{M}$   $\alpha_3\text{DH}_3$ , 5  $\mu\text{M}$   $\text{ZnSO}_4$ , 50 mM HEPES).

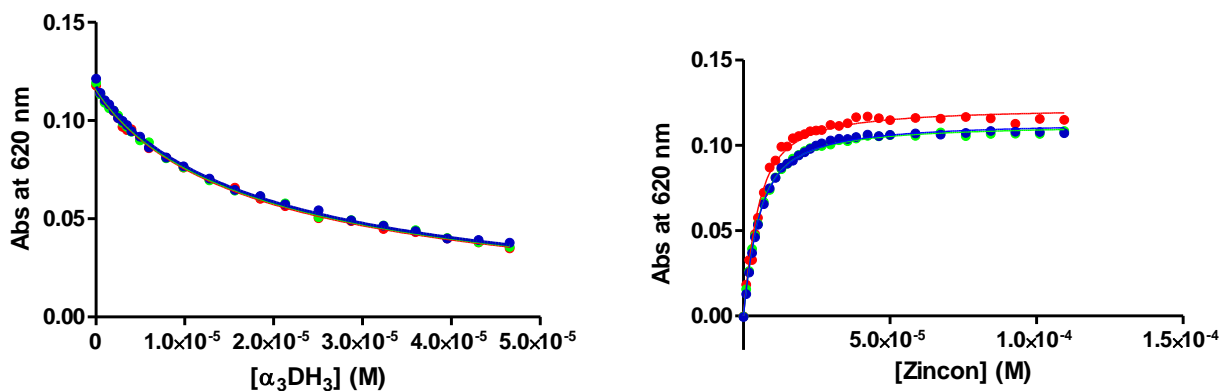


**Figure S3.** Competitive Zincon binding titrations at pH 9.0 with  $\alpha_3\text{DH}_3$ . In triplicate, plots show the absorbance of Zn(II)-Zincon at 620 nm plotted against the titrant concentration. Left: Titration of  $\alpha_3\text{DH}_3$  into Zn(II)-Zincon ( $10 \mu\text{M}$  Zincon,  $5 \mu\text{M}$   $\text{ZnSO}_4$ ,  $50 \text{mM}$  CHES). Right: Titration of Zincon into Zn(II) $\alpha_3\text{DH}_3$  ( $10 \mu\text{M}$   $\alpha_3\text{DH}_3$ ,  $5 \mu\text{M}$   $\text{ZnSO}_4$ ,  $50 \text{mM}$  CHES).

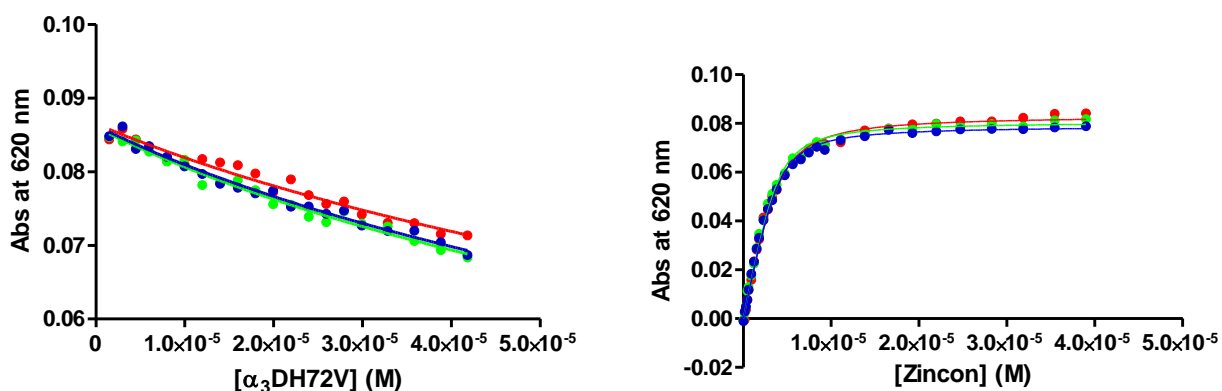


**Figure S4.** Competitive Zincon binding titrations at pH 9.0 with  $\alpha_3\text{DH72V}$ . In triplicate, plots show the absorbance of Zn(II)-Zincon at 620 nm plotted against the titrant concentration. Left: Titration of  $\alpha_3\text{DH72V}$  into Zn(II)-Zincon ( $8 \mu\text{M}$  Zincon,  $4 \mu\text{M}$   $\text{ZnSO}_4$ ,  $50 \text{mM}$  CHES). Right: Titration of Zincon into Zn(II) $\alpha_3\text{DH72V}$  ( $40 \mu\text{M}$   $\alpha_3\text{DH72V}$ ,  $4 \mu\text{M}$   $\text{ZnSO}_4$ ,  $50 \text{mM}$  CHES).

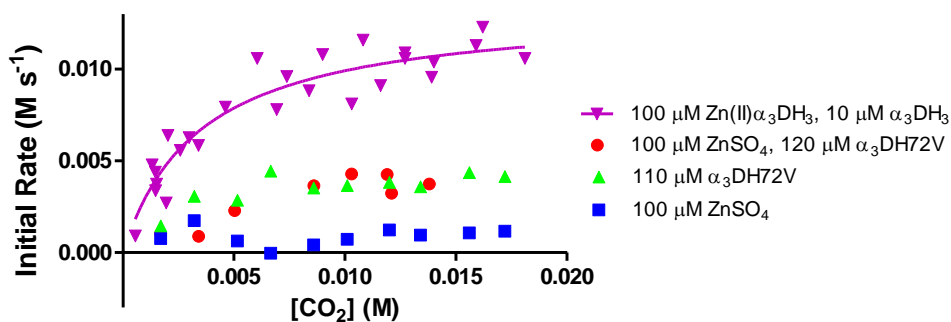


**Figure S5.** CO<sub>2</sub> hydration rates plotted versus substrate concentration at pH 9.5. The activity of Zn(II) $\alpha_3$ DH<sub>3</sub> (purple triangles) is significantly higher than any of the controls, showing that the activity results from the Zn(II)N<sub>3</sub>O site. Apo- $\alpha_3$ DH72V shows some activity (green triangles), but it is not enhanced by the addition of ZnSO<sub>4</sub> (red circles), showing that adventitiously-bound Zn(II) does not contribute to the activity. Free Zn(II) shows minimal activity (blue squares).

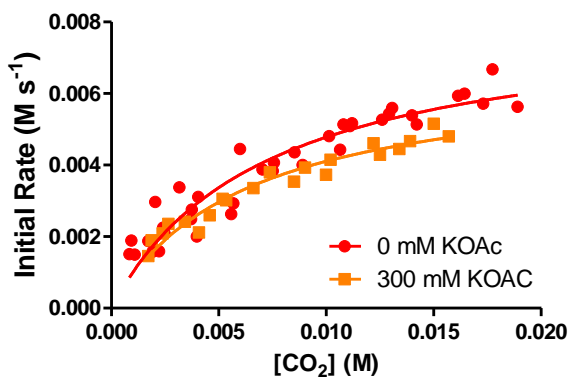


**Figure S6.** Michaelis-Menten plot for the hydration catalysis of CO<sub>2</sub> hydration by 100  $\mu$ M Zn(II) $\alpha_3$ DH<sub>3</sub> at pH 8.5 in the absence and presence of potassium acetate inhibitor.

**Table S1.** Kinetic parameters for the catalysis of CO<sub>2</sub> hydration by Zn(II) $\alpha_3$ DH<sub>3</sub> at pH 8.5 in the absence and presence of potassium acetate inhibitor.

| KOAc (mM) | $k_{\text{cat}}$ (s <sup>-1</sup> ) | $K_M$ (mM) | $k_{\text{cat}}/K_M$ (M <sup>-1</sup> s <sup>-1</sup> ) |
|-----------|-------------------------------------|------------|---|
| 0         | 82 ± 6                              | 7.2 ± 1.1  | 11,400 ± 1,100  |
| 300       | 67 ± 4                              | 6.2 ± 0.8  | 10,700 ± 800  |

## Experimental Section

### Expression and Purification of $\alpha_3\text{DH}_3$

The synthetic DNA for  $\alpha_3\text{DH}_3$  was cloned into a pET-15b vector (Celtek Genes) and expressed in *E. coli* BL21(DE3) competent cells (Invitrogen) in self-inducing media. The cells were lysed by sonication and the soluble protein was isolated after heat denaturation (55 °C) and acidification to pH 1.9. The lyophilized powder was redissolved and purified using reverse-phase HPLC with a linear gradient of H<sub>2</sub>O to 9:1 CH<sub>3</sub>CN/H<sub>2</sub>O over 50 minutes. All HPLC solvents contained 0.1% trifluoroacetic acid. The purified protein had a yield of 230 mg/L and a molecular weight of 8283.5 Da by ESI-MS (collected on a Micromass LCT Time-of-Flight Mass Spectrometer). This compares well to the calculated mass of 8283.1 Da for  $\alpha_3\text{DH}_3$  lacking formyl-methionine. The concentration of the protein was determined by measuring the absorbance at 280 nm using the measured molar extinction coefficient of 7849 mol<sup>-1</sup>cm<sup>-1</sup>.

### Expression and Purification of $\alpha_3\text{DH72V}$

Using the GeneArt® Site-Directed Mutagenesis System (Invitrogen), the codon for His72 was mutated to that for Val within the  $\alpha_3\text{D}$  gene (pET-15a vector). The resulting plasmid was expressed and purified as described above with a yield of 100 mg/L. The molecular weight of the pure protein was determined to be 7938.4 Da by ESI-MS, which compares well to the calculated mass of 7938.9 Da for  $\alpha_3\text{DH72V}$  lacking formyl-methionine.

### Circular Dichroism (CD) Spectroscopy

CD spectra were collected on an Aviv 202 CD Spectrometer at 25 °C using 1 cm path length open top quartz cuvettes. Samples were prepared at pH 9.0 in 10 mM potassium phosphate (ion source) and contained either 5  $\mu\text{M}$  peptide or 5  $\mu\text{M}$  peptide and 15  $\mu\text{M}$  ZnSO<sub>4</sub>. The percent folding was based on the presence of 59 helical residues and was determined using previously reported procedures.<sup>1,2</sup> Guanidine hydrochloride (GuaHCl) titrations were carried out using a Microlab 500 series syringe-pump automatic titrator controlled by Aviv software. Into a solution of 5  $\mu\text{M}$   $\alpha_3\text{DH}_3$  or 5  $\mu\text{M}$  Zn(II)- $\alpha_3\text{DH}_3$  in 10 mM KPhos at pH 9.0, GuaHCl was titrated to a concentration of 6.5 M, while keeping the protein concentration constant. The change in molar ellipticity upon titration was fit to a two-state unfolding model.<sup>3</sup>

### Zn(II) Binding Constant Determination

The dissociation constants for Zn(II) to  $\alpha_3\text{DH}_3$  and  $\alpha_3\text{DH72V}$  were determined at pH 7.5 and 9.0 at 25 °C following our previously reported procedures.<sup>4</sup>

### CO<sub>2</sub> Hydration Kinetics

The initial rates for CO<sub>2</sub> hydration catalyzed by Zn(II)- $\alpha_3\text{DH}_3$  were measured at 25.0 °C on an OLIS RSM Stopped Flow Spectrophotometer using Khalifah's changing pH-indicator method.<sup>5</sup> The substrate stock solution was prepared by bubbling CO<sub>2</sub> (Matheson Tri-Gas, Inc., Research Grade) through deionized water for at least 20 minutes and then diluted with deionized water in a gas-tight syringe. This substrate solution was mixed by the stopped-flow with either a control solution (containing only buffer, indicator, and apo- $\alpha_3\text{DH}_3$ ) or a catalyst solution (containing buffer, indicator, Zn(II)- $\alpha_3\text{DH}_3$ , and apo- $\alpha_3\text{DH}_3$ ). After 1:1 mixing with the substrate solution, each shot contained 50 mM buffer and 25  $\mu\text{M}$  indicator and were maintained at 0.1 M ionic strength with Na<sub>2</sub>SO<sub>4</sub>. Typically, the control shots contained 10  $\mu\text{M}$  apo- $\alpha_3\text{DH}_3$ , while the catalyst shots contained 110  $\mu\text{M}$   $\alpha_3\text{DH}_3$  and 100  $\mu\text{M}$  ZnSO<sub>4</sub>, ensuring a final Zn(II)- $\alpha_3\text{DH}_3$  concentration of 100  $\mu\text{M}$ . The buffer indicator pairs used were TAPS/*m*-cresol purple (pH 8-8.75,  $\lambda = 578$  nm,  $\Delta\epsilon = 35,000$  M<sup>-1</sup>cm<sup>-1</sup>), AMPSO/thymol blue (pH 8.75-9.25,  $\lambda = 590$  nm,  $\Delta\epsilon = 40,500$  M<sup>-1</sup>cm<sup>-1</sup>), and CHES/thymol blue (pH 9.25-9.5,  $\lambda = 590$  nm,  $\Delta\epsilon = 40,500$  M<sup>-1</sup>cm<sup>-1</sup>). The experimental buffer factors

were close to those which were calculated theoretically, allowing for the CO<sub>2</sub> concentrations to be checked throughout the experiment.<sup>5</sup> Upon rapid mixing of the substrate solution with the buffer/indicator solution by the stopped-flow spectrophotometer, several seconds of absorbance data was collected. Initial rates were determined from the initial linear portion of the reaction (usually less than the first 10%). The rates from 6-11 replicates were averaged and, at each substrate concentration, the rate for the control solution was subtracted from that of the catalyst. The difference, reflecting the initial rate of the catalyst, was plotted as a function of [CO<sub>2</sub>] and fitted using the Michaelis-Menten equation (in GraphPad Prism 5). Inhibition experiments were carried out as described above, with the addition of 300 mM KOAc to the buffer/indicator solution at pH 8.5.

## EXAFS

Samples for EXAFS were prepared with final concentrations of 1 mM ZnSO<sub>4</sub>, 1.5 mM α<sub>3</sub>DH<sub>3</sub>, 50 mM CHES buffer, and 4.1 M glycerol at pH 9.0. At these concentrations, >99.9% of the Zn(II) is bound to α<sub>3</sub>DH<sub>3</sub>. The samples were rapidly frozen in liquid N<sub>2</sub> and maintained at ~10K throughout the measurements. EXAFS data were measured at SSRL Beamline 7-3 using a Si(220) double crystal monochromator and a Rh-coated vertically collimating harmonic rejection monochromator. Data were measured as fluorescence excitation spectra using a 30-element energy-resolving Ge detector. Data were collected using 10 eV steps in the pre-edge region (9350 - 9640 eV), 0.25 eV for the edge region (9640 - 9690 eV), and 0.05 Å<sup>-1</sup> increments for the extended x-ray absorption fine structure (EXAFS) region to  $k=13$  Å<sup>-1</sup>, with integration times of 1 s in the pre-edge and edge regions and 1-20 s ( $k^3$  weighted) in the EXAFS region for a total scan time of ~40 min.

Raw data were converted to EXAFS and fit using the EXAFSPAK<sup>6</sup> suite of programs, with theoretical amplitude and phase parameters calculated using FEFF<sup>9</sup> using two metal-ligand distances, the Debye-Waller factors for the Zn-O and Zn-histidine shells ( $1.6 \times 10^{-3}$  Å<sup>2</sup> and  $5.6 \times 10^{-3}$  Å<sup>2</sup>, respectively) and ΔE0 (-8.3 eV) as the only adjustable parameters. The remaining histidine distances assuming a rigid imidazole ring with distances and angles equal to the average of Zn-histidine models found in the Cambridge Crystallographic database and the imidazole Debye-Waller factors were defined by assuming that the σ<sup>2</sup> value for each scattering path increased proportionally from those calculated by Bunker and Dimakis for an ordered imidazole.<sup>8</sup>

## References

- (1) Luo, P.; Baldwin, R. L. *Biochem.* **1997**, *36*, 8413–8421.
- (2) Rohl, C. A.; Baldwin, R. L. *Biochem.* **1997**, *2960*, 8435–8442.
- (3) Santoro, M. M.; Bolen, D. W. *Biochemistry* **1988**, *27*, 8063–8068.
- (4) Zastrow, M. L.; Pecoraro, V. L. *J. Am. Chem. Soc.* **2013**, *135*, 5895–5903.
- (5) Khalifah, R. G. *J. Biol. Chem.* **1971**, *246*, 2561–2573.
- (6) George G. N.; Pickering, I. J. <http://ssrl.slac.stanford.edu/~george/exafspak/exafs.htm>.
- (7) Rehr, J.J.; Kas, J. J.; Vila, F. D.; Prange, M. P.; Jorissen, K. *Phys. Chem. Chem. Phys.* **2010**, *12*, 5503–5513.
- (8) Dimakis, N.; Bunker, G. *Phy. Rev. B* **2002**, *65*, 201103.